

A counterintuitive method for slowing down an analyte in a nanopore by reversing the pore voltage and increasing analyte mobility

G. Sampath

P. B. 7849, J. P. Nagar P. O., Bengaluru-560078, India

Abstract. A major obstacle faced by nanopore-based polymer sequencing and analysis is the high speed of translocation of an analyte (nucleotide, DNA, amino acid (AA), peptide) through the pore; the rate currently exceeds available detector bandwidth. Except for one method that uses an enzyme ratchet to sequence DNA, attempts to resolve the problem satisfactorily have been largely unsuccessful. Here a counterintuitive method based on *reversing the pore voltage*, and, with some analytes, *increasing their mobility*, is described. A simplified Fokker-Planck model shows a significant increase in translocation times for single nucleotides and AAs (up from ~10 ns to ~1 ms). More realistic simulations show that with a bi-level positive-negative pore voltage profile all four nucleotides in DNA (dAMP, dTMP, dCMP, and dGMP) and the 20 proteinogenic amino acids can be trapped inside the pore long enough for detection with bandwidths of ~1-10 KHz.

Keywords: nanopore; translocation slowdown; mobility; polymer sequencing; bandwidth; diffusion

1. Introduction

In recent years nanopores have emerged as a potential alternative to established and developing methods of polymer sequencing and analysis [1]. Nanopore sequencing is based on translocating a polymer through a nano-sized pore in an electrolytic cell (e-cell) and using the size of the resulting current blockade to identify successive monomers. Increasingly, nanopores are becoming a viable alternative for DNA sequencing [2]. In contrast nanopore protein sequencing is yet to show the same level of success [3]. Methods reported include theoretical models [4,5], practical investigations [6-8], and molecular dynamics simulations [9].

The nanopore approach faces three major problems: 1) The polymer translocates through the pore at a higher rate than can be handled by the detector; 2) It is hard to distinguish among monomers based on just the blockade level, as more often than not different monomers are physically and/or chemically similar and measured differences are slight; this is more so with AAs, of which there are 20, compared to four bases with DNA; 3) The blockade level has to be higher than the noise picked up by the detector. An effective solution to the first problem will also reduce high frequency noise, which serves to mitigate the third problem. A range of slowdown methods have been reported [10-17]. The last of these [17] has been used in DNA sequencing; it is based on the use of an enzyme motor that acts as a ratchet to slow down a strand of DNA and enables synthesis of the complementary strand. The primary aim in most of these methods is to allow discrimination of bases in DNA and residues in proteins. However other than the solution in [17], which is limited to the sequencing by synthesis (SBS) method, the problem remains truculent and continues to resist general solution. The second problem, namely separation of the 20 AAs in measurement, is addressed later when introducing a method for AA identification that is designed to achieve such separation and make physical and chemical differences less of a problem [18]. A fourth, less severe, problem is that of delivering the analyte from the top of the *cis* chamber of the e-cell to the pore entrance. One recent solution to this is based on the use of nanopipettes to deliver single molecules to desired locations [19].

The present work

A method for slowing down an analyte in a nanopore that is based on reversing the voltage across the pore and, as appropriate, increasing the mobility of the analyte, is introduced. This is the opposite of conventional methods, which may be aimed at decreasing (but not reversing) the voltage and/or decreasing analyte mobility; for example, the latter may be achieved with a high viscosity solution. A simplified Fokker-Planck model of analyte translocation is used to show that significant increases in translocation times, up from tens of nanoseconds to about a millisecond, for any of the four nucleotides or the 20 AAs, are possible. This conclusion is reinforced by numerical simulations. Following this development a method of separation of the 20 AAs that uses cognate tRNAs is described; this effectively turns analyte blockade measurement from a high-precision analog problem into a low-precision digital one. The problem of delivering the analyte to the pore entrance is shown to be amenable to the use of hydraulic pressure, which also ensures that the analyte does not regress into *cis* and diffuse away.

2. A Fokker-Planck model of analyte translocation through a nanopore.

Consider an e-cell with *cis* and *trans* chambers filled with an electrolyte (like KCl) and separated by a thin membrane containing a nano-sized pore (Figure 1a). When a voltage V (*cis* negative to *trans* positive) is applied across the membrane the electrolyte is ionized; K^+ ions flow from *trans* to *cis* and Cl^- ions from *cis* to *trans* through the pore. An analyte molecule introduced into *cis* will flow in a direction based on the electrical charge it carries. Thus the four nucleotides dAMP, dTMP, dCMP, and dGMP that make up DNA are negatively charged and go from *cis* to *trans*. In comparison the 20 amino acids carry different amounts of charge, varying from 0 to ± 2 , depending on the pH level of the solution. The exact value of the charge can be calculated with the Henderson-Hasselbalch (H-H) equation [20]. In the absence of a transmembrane voltage all analytes diffuse through the solution, with the direction of transport determined by boundary conditions. For example, if the top wall of *cis* is reflective then an analyte in *cis* will diffuse through the pore and end up in *trans*. The presence of a superimposed voltage V biases the motion in the direction of the electric field. Analyte motion can be modeled mathematically with a Fokker-Planck (F-P) equation. Such models have been widely used in the study of DNA and peptide translocation through a nanopore. Here,

an F-P equation is used to model the e-cell in Figure 1a and used to compute the dwell/translocation time of an analyte in/through the pore. Only the essential features of the model are given here, a detailed treatment can be found in the Supplement to [4].

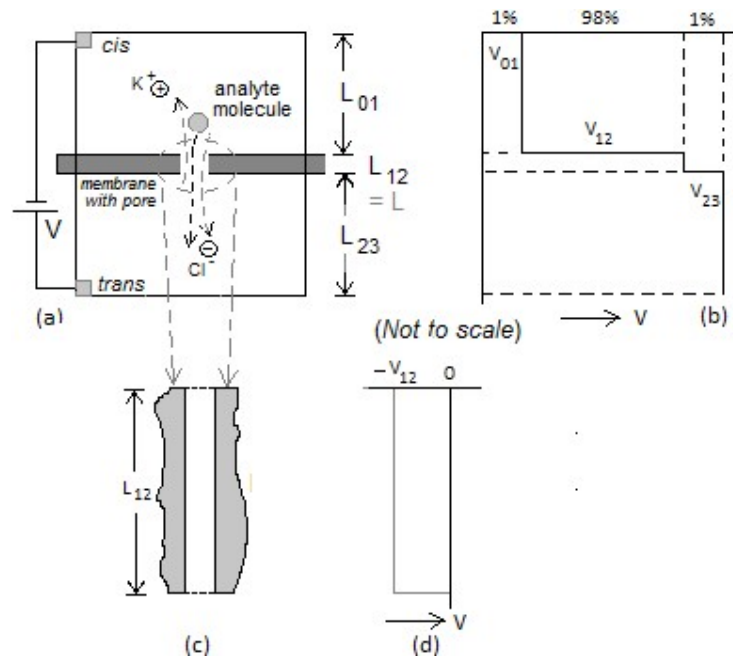


Fig. 1 Schematic of electrolytic cell (e-cell); membrane containing nanopore separates *cis* and *trans* chambers containing salt (KCl) solution. (a) Ionic current flow in e-cell is due to K^+ and Cl^- ions; analyte translocating through pore causes reduction of open pore current; (b) 98% of voltage V applied between *cis* and *trans* drops across pore; (c) Enlarged view of pore of length L_{12} ; (d) Negative V across pore in (c)

To start with, a one-dimensional approximation is applied to the nanopore in Figure 1a over the segment $0 \leq z \leq L_{12}$ over time $t \geq 0$. An analyte is assumed to be a particle that is released at $z = 0$, $t = 0$; reflected at $z = 0$, $t > 0$; and captured at $z = L_{12}$, $t > 0$. The trajectory of the analyte as it passes through the pore is described by the function $G(z,t)$:

$$\partial G / \partial t + v_z \partial G / \partial z = D \partial^2 G / \partial z^2, \quad z \in [0, L_{12}] \quad (1)$$

with the following initial and boundary value conditions:

1) The particle is released at $z = 0$ and time $t = 0$:

$$G(0, t=0) = \delta(z) \quad (2)$$

2) The particle is captured at $z = L$:

$$G(L, t) = 0 \quad (3)$$

3) The particle is reflected at $z = 0$:

$$D \partial G(z, t) / \partial z |_{z=0} = v_z G(z, t) \quad (4)$$

Here D is the diffusion constant; v_z , the drift velocity through the pore, is given by $v_z = \mu V_{12} / L$, where μ is the analyte mobility. D and μ are physical constants that are given by the following equations:

$$D = k_B T_R / 6\pi\eta R_{hyd} \quad \mu = C_{mult}q / 6\pi\eta R_{hyd} \quad (5 \text{ a,b})$$

Here k_B is the Boltzmann constant (1.3806×10^{-23} J/K), T_R is the room temperature (298° K), η is the solvent viscosity (0.001 Pa.s for water), R_{hyd} is the hydrodynamic radius of the analyte molecule (Å), q is the electron charge (-1.619×10^{-19} coulomb), and C_{mult} is the charge multiplier for the analyte. C_{mult} depends on the solution pH, it is calculated with the H-H equation and is applied only to AAs; for nucleotides its value is taken as 1 at pH = 7. Table 1 shows charge values for all 20 amino acids for solution pH = 7, 9, and 11. The 20 AAs can be divided into six equivalence classes based on their charge multipliers:

$$\text{AA} = \{ \{A, N, Q, G, I, L, M, F, P, S, T, W, V\}, \{R, K\}, \{D, E\}, \{C\}, \{H\}, \{Y\} \} \quad (6)$$

Two AAs are in the same class if their charge multipliers are the same or nearly so.

Table 1. Charge multipliers for the 20 AAs at different pH values.

pH	A	R	N	D	C	Q	E	G	H	I
7	-0.002	0.998	-0.002	-1.001	-0.047	-0.002	-1.000	-0.002	0.089	-0.002
9	-0.170	0.830	-0.170	-1.170	-0.993	-0.170	-1.170	-0.170	-0.169	-0.170
11	-0.953	0.015	-0.953	-1.953	-1.951	-0.953	-1.953	-0.953	-0.953	-0.953
pH	L	K	M	F	P	S	T	W	Y	V
7	-0.002	0.998	-0.002	-0.002	-0.002	-0.002	-0.002	-0.002	-0.003	-0.002
9	-0.170	0.802	-0.170	-0.170	-0.170	-0.170	-0.170	-0.170	-0.248	-0.170
11	-0.953	-0.700	-0.953	-0.953	-0.953	-0.953	-0.953	-0.953	-1.848	-0.953

Let T be the time of translocation of an analyte through the pore and E(T) its mean. Routine analysis of Equations 1-4 gives

$$E(T) = (L^2/\mu V_{12})[1 - (1/\alpha)(1 - e^{-\alpha})], \quad \alpha \neq 0 \quad (7a)$$

$$= L^2/2D, \quad \alpha = 0 \quad (7b)$$

$$\alpha = v_z L/D = \mu V_{12}/D \quad (8)$$

Equation 7b corresponds to pure diffusion ($\alpha = 0$). There are three non-diffusion cases:

Case 1: $\alpha \neq 0$ and $|\alpha|$ is small. On using the approximation $e^{-\alpha} = 1 - \alpha + \alpha^2/2 - \alpha^3/6 + \dots$

Equation 7a reduces to

$$E(T) = E(T) \approx (L^2/2D)(1 - \alpha/3) \quad (9)$$

The first term is the mean translocation time under pure diffusion. With voltage $V \neq 0$ it is reduced by $|\alpha|/3$ when $\alpha > 0$ and increased by $|\alpha|/3$ when $\alpha < 0$. Thus with small α diffusion dominates the translocation time. From Equations 7a and b, μ and D are both inversely proportional to η so α does not change with the increase in η . This means that increasing the viscosity of the solution cannot increase the translocation time appreciably. Any such increase can only be due to μ in the denominator of the right side of Equation 7a; practical reductions in μ are typically one to two orders of magnitude [12-14].

Case 2: $\alpha \gg 0$. In this case $e^{-\alpha} \rightarrow 0$ and Equation 7a reduces to

$$E(T) \rightarrow L^2/2D \quad (10)$$

which corresponds to pure diffusion.

Case 3: $\alpha \ll 0$. This is the most interesting case because it breaks the grip that diffusion has on analyte speed. With large negative α the exponential term $e^{-\alpha}$ ($= e^{|\alpha|}$) dominates the factor inside the square brackets on the right side of Equation 7a. One can then write

$$E(T) \approx (L^2/\mu V) e^{|\alpha|/|\alpha|} \quad (11)$$

or

$$E(T) \approx (L^2/D\mu^2 V^2) e^{|\mu V/D|} \quad (12)$$

The latter shows that with a linear increase in μ the $e^{|\alpha|}$ term in the numerator increases exponentially, while the denominator increases only as μ^2 . Thus reversing V and increasing μ can, in theory drastically increase the translocation time.

Table 2 shows translocation times for four nucleotides (dAMP, dTMP, DCMP, and dGMP) for a nanopore of length 10 nm and diameter 3 nm. In the table the shaded backgrounds turn lighter as translocation times increase.

Table 2. Translocation times for 4 of the 5 nucleotides for different pore voltages, positive and negative. Gray level of background of data cells decreases with increasing translocation times.

Trans-membrane voltage	Translocation time through pore			
	dAMP	dTMP	dCMP	dGMP
-0.5	42.2 ms	41.3 ms	60.9 ms	42.4 ms
-0.4	1.34 ms	1.32 ms	1.78 ms	1.35 ms
-0.3	48.6 μ s	47.7 μ s	59.1 μ s	49.0 μ s
-0.2	2.22 μ s	2.18 μ s	2.48 μ s	2.24 μ s
0	27.9 ns	27.5 ns	27.5 ns	28.3 ns
0.2	6.25 ns	6.17 ns	6.05 ns	6.35 ns
0.3	4.37 ns	4.31 ns	4.22 ns	4.44 ns
0.4	3.36 ns	3.31 ns	3.24 ns	3.41 ns
0.5	2.72 ns	2.68 ns	2.63 ns	2.76 ns

Table 3 shows translocation times for six of the 20 AAs for different values of V and pH. The AAs in the first column of the table represent their equivalence class. The pH value and voltage required to raise translocation times to the millisecond range are shaded.

Table 3. Translocation times of analytes as a function of solution pH, analyte mobility, and negative pore voltage. Cases in which translocation times are in the millisecond range are shown with gray background.

Analyte	Solution pH	Mobility (m^2/Vs)	V (volt)	Translocation time (ms) through pore	V (volt)	Translocation time (ms) through pore
dAMP	7	1.74×10^{-8}	0.4	3.36×10^{-6}	-0.4	1.34
Alanine	11	3.05×10^{-8}	0.5	1.55×10^{-6}	-0.5	10.2
Arginine	7	-2.36×10^{-8}	0.5	30.00	-0.5	2.01×10^{-6}
Aspartic Acid	7	2.82×10^{-8}	0.5	1.68×10^{-6}	-0.5	26.6
Cysteine	9	2.95×10^{-8}	0.5	1.61×10^{-6}	-0.5	22
Histidine	11	2.32×10^{-8}	0.5	2.04×10^{-6}	-0.5	13.3
Tyrosine	11	4.4×10^{-8}	0.3	1.81×10^{-6}	-0.3	209

3. A bi-level voltage profile to trap an analyte for extended periods of time

The F-P model above considers the pore in isolation and assumes that it is reflective on the inside. The pore, however, is an integral part of an e-cell to which an analyte is added at the top of the *cis* chamber; the latter behaves like a reflective boundary. With V set to the normal polarity (*cis* negative, *trans* positive), a negatively charged analyte diffuses through *cis* to the pore entrance, thereafter it translocates through the pore into *trans*. This latter behavior can be viewed as if the analyte originated from the top of the pore; the translocation time is then given by Equation 7 with $\alpha > 0$ above (Case 1). This time is the usual low one of the order of a few (10-100) nanoseconds and is normally beyond the capability of the detector.

In what follows, the analyte is assumed to be negatively charged (for example dAMP or glutamic acid). The development can be carried over to positively charged analytes (such as arginine or cysteine) with a systematic change of sign.

Now consider reversing the voltage across the pore. For the F-P model to be applicable, two conditions need to be satisfied:

Condition 1: The analyte must translocate to the entrance of *cis* without being lost to diffusion and enter the pore; and

Condition 2: The pore entrance must behave, at least approximately, like a reflector to an analyte (Equation 4) after the latter enters the pore, and the analyte should not regress into *cis* and diffuse away.

Condition 2 can be written in two parts:

2a: The analyte must be able to enter the pore before it experiences the decelerating effect of a negative electric field.

2b: After entering the negative field the analyte must remain inside the pore for a sufficiently long time to allow its detection; this is contingent on *2a* being satisfied.

For now assume that Condition 1 can be satisfied by using an appropriate method to drive the analyte into the pore; this aspect is discussed later. Consider what happens when a negative voltage is applied across the full pore. At the *cis*-pore boundary: the analyte experiences a strong negative electric field inside the pore and a much weaker one in *cis*. As a result the analyte will not be able to go too far into the interior of the pore.

However both 2a and 2b can be satisfied if a bi-level pore voltage is used with normal polarity over the pore segment $[0, aL]$, $0 \leq a < 1$, and the opposite polarity over $[0, (1-a)L]$, with appropriate values of a and V . Figure 2 shows such a voltage profile. Notice that the analyte is only required to be inside the pore for a sufficiently long time, it is not necessary that it fully translocate through the pore into *trans*. In the latter case, following detection the analyte can always be pushed out with an appropriate value of voltage, and the next analyte transferred into *cis*.

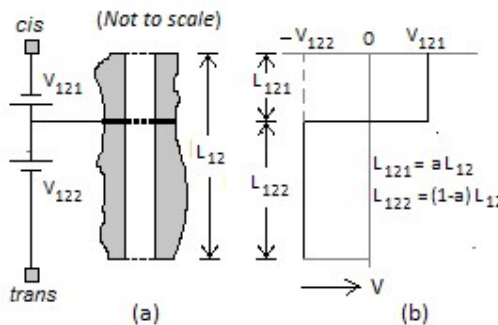


Fig. 2 (a) Two pores in tandem with different voltages across each; (b) Positive voltage V_{121} across pore of length $L_{121} = aL_{12}$, negative voltage V_{122} across pore of length $L_{122} = (1-a)L_{12}$; $0 \leq a \leq 1$.

As the simulations below show, there is considerable deviation from this ideal model because the top of the pore is not an ideal reflector but a leaky one. As a result there is a considerable amount of oscillation at the *cis*-pore boundary, which reduces the dwell time inside the pore. Nevertheless, as discussed above, with a suitable change in the voltage profile the desired slowdown can be obtained. Thus what is needed is a force that moves the analyte away from the *cis*-pore boundary and far enough into the pore that the dwell time inside is increased considerably. The next section shows that with the voltage profile in Figure 2 with $a = 0.5$ and suitable values of V_{121} and $-V_{122}$ can trap the analyte inside the pore for from 0.1 to 1 ms. A detection bandwidth of just a few (1-10) KHz would then be sufficient to detect the trapped analyte.

4. Simulation experiments and results

The slowdown process described above was simulated by assuming an analyte molecule to be a dimensionless particle. Figures 1a and 2a show schematics of the structures simulated; in Figure 2a the length of the pore over which the voltage changes from positive to negative is assumed to be negligible compared to the length of the tandem pore. The simulation procedure is similar to that in [21], which simulates translocation of free nucleotides through a tandem pore [4]. In the latter the terminal residue of a DNA strand passing through the first pore of a tandem electrolytic cell is cleaved by an exonuclease on the exit side of the pore, enters and translocates through a second nanopore, and is identified by the level of the blockade caused in the second pore.

To assess the efficacy of slowdown when using negative pore voltages or a two-level voltage profile a number of parameters were used (diffusion coefficient, mobility, hydraulic pressure level, origin of particle, and number of diffusion steps). The following measures are computed: 1) Dwell time inside the pore; 2) Time to translocate through the pore (without having regressed into *cis* after entering the pore); and 3) Frequency of dwell times for each time decade in the range 10^{-9} s to 10^{-3} s (that is, 10^{-9} s, 10^{-8} s, ..., 10^{-3} s). The simulation is stopped when the number of time steps reaches 2×10^9 , which corresponds to an experiment run time of 2 ms with a time step of 10^{-12} s. The following analytes were used: 1) dAMP, 2) Arginine, and 3) Alanine (with two different values of pH). dAMP represents all five nucleotides, Arginine the AA subset {R, K, D, E}, and Alanine the AA subset {A, N, Q, G, I, L, M, F, P, S, T, W, V}. For convenience all analytes were assumed to be negatively charged in the simulation and drawn from *cis* to *trans* through the pore by a normal positive voltage. With positively charged analytes it is only necessary to change the sign of the mobility value μ and of the *cis* and *trans* voltages; with the bi-level voltage the signs of the two levels are flipped. The results are not materially affected in any way.

Table 4 below shows the translocation time and maximum dwell time for the three analytes with three different positive and three different negative values of the pore voltage. While reversing the voltage does result in an increase in the dwell/translocation time in almost all cases, the maximum time is still under 1 μ s, which is not sufficient.

Table 4. Translocation time of analyte through pore and maximum dwell time of analyte in pore for different pore voltages, positive and negative

	dAMP (pH=7)	Arg (pH=7)	Ala (pH=7)	Ala (pH=11)

V (volt)	translocation time (10^{-12} s)	maximum dwell time (10^{-12} s)	translocation time (10^{-12} s)	maximum dwell time (10^{-12} s)	translocation time (10^{-12} s)	maximum dwell time (10^{-12} s)	translocation time (10^{-12} s)	maximum dwell time (10^{-12} s)
0.1	23499	3861	50815	7404				
0.3	9106	133	22089	241				
0.5	11905	23	30270	8	35357	438	6643	107
-0.1	67701	43757	74564	150879				
-0.3	10038	32632	20098	135080				
-0.5	(still inside pore)	13383	13578	162811	26903	18369	(still inside pore)	17183

As noted above the remedy is to use a two-level voltage profile with positive and negative segments. Figure 3 shows dwell or translocation times for the four analytes with two such profiles. When an analyte finds itself in the pore under the influence of the bilevel pore voltage (two combinations of positive and negative voltage are used) it may oscillate between *cis* and the pore, stay for extended times inside the pore, or translocate fully to exit into *trans*. In the last case it could regress back into the pore; however in the simulation runs the run was terminated when the analyte exited into *trans*. As noted above, when no translocation occurs a run is terminated when the total number of steps reaches 2×10^9 . When translocation occurs the larger of the dwell time and the translocation time through the pore is used as the measure of slowdown. In the absence of full translocation the longest dwell time of the analyte during the simulation run is used. Full translocation is not a requirement in the model of analyte detection/identification used here. Thus where there is no full translocation and exit into *trans*, an analyte could remain trapped inside the pore for sufficiently long times that the detector can detect the occurrence of a blockade in the pore current and measure the size of the blockade with adequate measurement precision.

Note the jump in dwell/translocation time for Alanine by about 4 orders of magnitude when the solution pH is changed from 7 to 11, which results in its mobility increasing by more than two orders of magnitude (see Table 1).

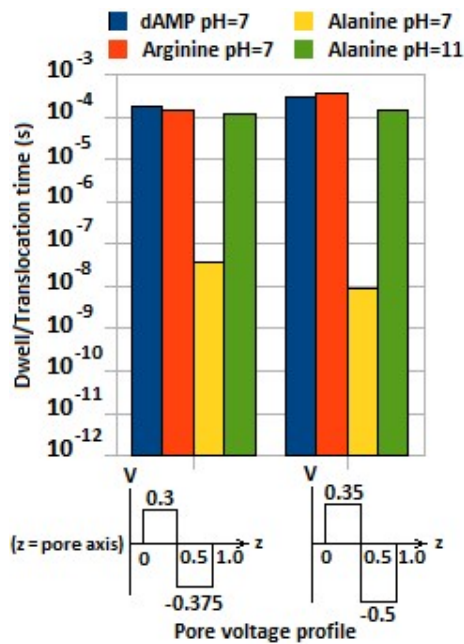


Fig 3. Histogram chart showing dwell or translocation time of analytes for two pore voltage profiles. Time data correspond to larger of dwell time and translocation time through pore.

5. Discussion

1. The method presented is fairly straightforward as it does not require any special devices or chemicals. The only special requirement is that a tandem of two pores be used with a metallic join between for a terminal connection. This can be done more easily with solid-state pores than with biological pores. Furthermore, pore voltages can be higher with the former, whereas with a biological pore they are limited to about 300 mV, which is too low according to Equation 7 to allow drastic slowdowns. This is also borne out by the simulation results in Table 4.

2. With AAs since different pH values are used to achieve slowdown, they need to be probed in different e-cells. A method to separate AAs from a sample by routing them to 20 different e-cells (one for each of the 20 different AAs) is described in [18]. The following is a brief summary.

Separation is based on the superspecificity property of tRNAs [22], which is used by living cells to accurately translate mRNA to protein. Thus for every amino acid (AA) there is a tRNA that binds to it and to no other (the *in vitro* error rate is $\sim 1/350$) [23]. Binding is accompanied by the release of adenosine monophosphate (AMP). In the method introduced in [18] an AA is fed into a micro-sized reservoir-cavity structure. An AA is bound by a cognate aminoacyl tRNA synthetase to its cognate tRNA in the cavity; the resulting charged (amino-acyl) tRNA is filtered out and deacylated. The freed AA is then identified through a current blockade caused in a nanopore. Measurement in this approach is limited to determining whether a current blockade occurs or not (the exact size of the blockade is not relevant), which gives it a binary character and digitizes the measurement process. The slowdown method described above can be used in each of the 20 cells to enable detection of a blockade with a bandwidth of a few KHz. As discussed in [18] each of the cells is isolated from the others so that a cell is like a silo in which the behavior of the analyte can be controlled independently based on the specific properties of the analyte. Thus, for example, the pore voltage can be set based on the volume of the analyte to maximize blockade size. Similarly the polarity of the voltage can be set based on the AA. For example, arginine has a positive charge at pH = 7, alanine is almost without charge at pH=7 but has a high negative charge at pH = 11. Identifying them in separate cells with different solution pH values makes the measurement process much simpler.

3. In nanopore studies it is usually assumed that an analyte finds its way to the pore entrance and is drawn into the pore by the pore voltage. In part entry is based on the pore's access resistance, which is the resistance due to the jump decrease in the diameter at the *cis*-pore boundary (which is reminiscent of water swirling before entering a drain). However analyte translocation is a stochastic phenomenon so there is no guarantee that such entry will occur within a reasonable amount of time. Several attempts to redress this situation have been reported. One of these [19] uses a nanopipette to trap short DNA strands for transfer to a detector like a nanopore. In the present case the narrow tube of the nanopipette can be positioned above the pore and the analyte molecule added to the mouth of the pipette.

Here a different approach based on the use of hydraulic pressure [24] is used. Thus a piston at the top of *cis* with a pressure of ΔP on it results in flow of the electrolyte to and through the pore. Assuming hydraulic flow to be Poiseuille flow, the velocities of the analyte in *cis* and pore are given by:

$$v_{\text{hyd}} = \Delta P R_{\text{cis}}^2 / 8\eta L_{\text{cis}} \quad (13a)$$

$$= \Delta P R_{\text{pore}}^2 / 8\eta L_{\text{pore}} \quad (13b)$$

The hydraulic flow velocity in *cis* is many times greater than that in the pore. Similarly it is negligible in the pore compared to the electrophoretic velocity due to the pore voltage. Simulations show that with this arrangement the analyte is always delivered to the pore. Table 5 summarizes the results.

Table 5. Translocation times for an analyte from the top of *cis* to the entrance of the pore for different hydraulic pressures

hydraulic pressure (atm)	translocation time (10^{-12} s)
1	151274
1.5	123181
2	99838
2.5	93712
3	78457

4. An analyte may be trapped multiple times inside the pore. Sufficiently long dwells can be recorded by the detector to increase the confidence level of the read. With n such dwells, such multiple reads can be thought of as providing nX coverage.

References

- [1] L. Reynaud, A. Bouchet-Spinelli, C. Raillon, and A. Buhot, "Sensing with nanopores and aptamers: a way forward", Sensors 20, 4495, 2020. doi:10.3390/s20164495
- [2] D. Deamer, M. Akeson, and D. Branton, "Three decades of nanopore sequencing". Nat. Biotechnol. 34, 518–524, 2016.
- [3] N. Callahan, J. Tullman, Z. Kelman, and J. Marino. "Strategies for development of a next-generation protein sequencing platform". Trends Biochem. Sci. 2019. doi:10.1016/j.tibs.2019.09.005.
- [4] G. Sampath. "Amino acid discrimination in a nanopore and the feasibility of sequencing peptides with a tandem cell and exopeptidase". RSC Adv. 5, 30694–30700, 2015.
- [5] P. Boynton and M. Di Ventra. "Sequencing proteins with transverse ionic transport in nanochannels". Sci. Rep. 6, 25232, 2016.
- [6] Y. Zhao, B. Ashcroft, P. Zhang, H. Liu, S. Sen, W. Song, J. Im, B. Gyarfas, S. Manna, S. Biswas, C. Borges, and S. Lindsay. "Single-molecule spectroscopy of amino acids and peptides by recognition tunneling". Nature Nanotechnol. 9, 466–473, 2014.

[7] E. Kennedy, Z. Dong, C. Tennant, and G. Timp. "Reading the primary structure of a protein with 0.07 nm³ resolution using a subnanometre-diameter pore". *Nature Nanotechnol.* 11, 968–976, 2016.

[8] H. Ouldali, K. Sarthak, T. Ensslen, F. Piguet, P. Manivet, J. Pelta, J. C. Behrends, A. Aksimentiev, and A. Oukhaled, "Electrical recognition of the twenty proteinogenic amino acids using an aerolysin nanopore", *Nature Biotech.*, 38, 176–181, 2020. doi: 10.1038/s41587-019-0345-2 (Reviewed in: S. Howorka and Z. S. Siwy, "Reading amino acids in a nanopore", *Nature Biotechnol.* 38, 159–160, 2020. doi: 10.1038/s41587-019-0401-y)

[9] W. Si, Y. Zhang, G. Wu, Y. Kan, Y. Zhang J. Sha, and Y. Chen, "Discrimination of Protein Amino Acid or Its Protonated State at Single-Residue Resolution by Graphene Nanopores", *Small*, 2019. doi: 10.1002/smll.201900036

[10] U. F. Keyser. "Controlling molecular transport through nanopores". *J. R. Soc. Interface* 8, 1369–1378, 2011.

[11] S. Carson and M. Wanunu. "Challenges in DNA motion control and sequence readout using nanopore devices". *Nanotechnology*, 26, 074004, 2015. doi:10.1088/0957-4484/26/7/074004

[12] R. Samanthi, S. de Zoysa, D. A. Jayawardhana, Q. Zhao, D. Wang, D. W. Armstrong, and X. Guan. "Slowing DNA translocation through nanopores using a solution containing organic salts". *J. Phys. Chem. B* 113, 13332–13336, 2009.

[13] S. W. Kowalczyk, D. B. Wells, A. Aksimentiev, and C. Dekker. "Slowing down DNA translocation through a nanopore in lithium chloride". *Nano Lett.* 12, 1038–1044, 2012. doi:1 0.1021/nl204273h

[14] J. Feng, K. Liu, R. D. Bulushev, S. Khlybov, D. Dumcenco, A. Kis, and A. Radenovic. "Identification of single nucleotides in MoS₂ nanopores". *Nature Nanotech.*, 2015. doi: 10.1038/nnano.2015.219

[15] W. Si, Y. Zhang, J. Sha, and Y. Chen, "Controllable and reversible DNA translocation through a single-layer molybdenum disulfide nanopore", *Nanoscale*, 10, 19450–19458, 2018. doi: 10.1039/c8nr05830j

[16] J. Larkin, R. Henley, D. C. Bell, T. Cohen-Karni, J. K. Rosenstein, and M. Wanunu, "Slow DNA transport through nanopores in hafnium oxide membranes," *ACS Nano*, 7, 10121–10128, 2013.

[17] K. R. Lieberman, G. M. Cherf, M. J. Doody, F. Olasagasti, Y. Kolodji, and M. Akeson, "Processive replication of single DNA molecules in a nanopore catalyzed by phi29 DNA polymerase", *J. Am. Chem. Soc.* 132, 17961–17972, 2010. doi: 10.1021/ja1087612

[18] G. Sampath, "Label-free amino acid identification for de novo protein sequencing via tRNA charging and current blockade in a nanopore", *bioRxiv*, 2020.06.25.170803. doi:10.1101/2020.06.25.170803

[19] K. J. Freedman, L. M. Otto, A. P. Ivanov, A. Barik, S.-H. Oh, and J. B. Edel. "Nanopore sensing at ultra-low concentrations using single-molecule dielectrophoretic trapping". *Nature Commun.* 7, 10217, 2016. doi: 10.1038/ncomms10217

[20] D. L. Nelson and M. M. Cox, *Lehninger's Principles of Biochemistry*, 4th edn., 2005, W H Freeman.

[21] G. Sampath. "DNA sequencing with stacked nanopores and exonuclease: a simulation-based analysis". *Electrophoresis* 37, 2429–2434, 2016. doi: 10.1002/elps.201600049

[22] G. Bergtrom, *Cell and Molecular Biology*, 3rd edn. U. Wisconsin, 2018. https://dc.uwm.edu/biosci_facbooks_bergtrom/10

[23] D. Goodsell. "Aminoacyl-tRNA Synthetases". PDB Molecule of the Month, April 2001. doi:10.2210/rcsb_pdb/mom_2001_4

[24] B. Lu, D. P. Hoogerheide, Q. Zhao, H. Zhang, Z. Tang, D. Yu, and J. A. Golovchenko. "Pressure-controlled motion of single polymers through solid-state nanopores". *Nano Lett.* 13, 3048–3052, 2013.

Email: sampath_2068@yahoo.com